# Nonlinear Thermo-Elastic-Plastic and Creep Analysis by the Finite-Element Method

P. SHARIFI* AND D. N. YATES†
*Lockheed Missiles & Space Company, Inc., Sunnyvale, Calif.*

**Consistent with a Lagrangian displacement formulation, an incremental constitutive relation for uncoupled thermo-elastic-plastic and creep deformations is presented. The nonisothermal von Mises yield function and its associated flow rule are utilized, together with both isotropic and kinematic hardening rules. Steady-state creep deformations are considered using Norton-Odqvist's power law. This development is particularly applicable to the nonlinear finite element analysis of three-dimensional structures with time- and temperature-dependent material properties. Using a nonlinear general-purpose computer program which has been developed on the basis of this formulation, a number of numerical examples are solved and the results compared with the closed-form solutions.**

## Introduction

DURING the past two decades, an upsurge of interest has been generated for the nonlinear analysis of structural systems. The use of highly deformable structural elements, introduction of new materials, and their application at severe thermal and mechanical environments have been the main forces behind this growing interest.

Closed-form nonlinear solutions of complex structures undergoing large elastic-plastic and creep deformations present a formidable, if not impossible, task to the analyst. But modern numerical techniques together with the availability of high-speed computers have rendered the task a reality. One such method is the widely used discretization technique of finite elements. This method has been successfully applied to the solution of linear[1] and nonlinear[2] problems in structural mechanics.

Herein, in terms of three-dimensional Cartesian tensors, an incremental displacement formulation is presented for the nonlinear finite element analysis of structural systems undergoing large elastic, plastic, and creep deformations. Thermal effects and the variation of material properties as a function of time and temperature are also included in the derivations. Based on this formulation, a computer program (NEPSAP) has been developed which contains three-dimensional solids as well as two-dimensional bending and membrane elements. This program has been successfully applied to the nonlinear bending and buckling problems of complex geometries composed of a combination of the preceding types of elements.

However, lacking space, the presentation will be limited to the theoretical foundations of NEPSAP. Derivations of two- and three-dimensional element matrices used in NEPSAP and the organization of the program will not be discussed here.

## Kinematics

Figure 1 shows the motion of a three-dimensional body in its path of deformation. Three configurations are shown: $C_0$ (original or underformed configuration), $C_1$ (current deformed configuration), and $C_2$, a neighboring deformed configuration with respect to $C_1$. In terms of a fixed rectangular coordinate system, $z_i$, $z_i = z_i + {}^1u_i$, and $Z_i = z_i + {}^2u_i = z_i + u_i$ describe the positions of a generic material point in $C_0$, $C_1$, and $C_2$, respectively. Here, ${}^1u_i$, ${}^2u_i$ are components of total displacement vectors and $u_i = {}^2u_i - {}^1u_i$ (see Fig. 1). Throughout this work, left superscripts 1 and 2, respectively, denote configurations $C_1$ and $C_2$, and the incremental quantities between $C_1$ and $C_2$ have no left superscripts. Whenever indicial notations are used, summation convention applies and the Latin indices have a range of 1–3 while the Greek indices 1 and 2. Using Lagrangian definition, the strain tensors are given as

$$ {}^\alpha\varepsilon_{ij} = \tfrac{1}{2}\left[{}^\alpha u_{i,j} + {}^\alpha u_{j,i} + {}^\alpha u_{m,i}\,{}^\alpha u_{m,j}\right], \alpha = 1,2 \tag{1}$$

and

$$ \varepsilon_{ij} = e_{ij} + \eta_{ij} = {}^2\varepsilon_{ij} - {}^1\varepsilon_{ij} \tag{2}$$

where comma denotes differentiation with respect to the coordinates in $C_0$, i.e. $(\ )_{,i} = \partial/\partial z_i$, and

$$ 2e_{ij} = u_{i,j} + u_{j,i} + {}^1u_{m,i}\,u_{m,j} + u_{m,i}\,{}^1u_{m,j} \tag{3a}$$

$$ 2\eta_{ij} = u_{m,i}\,u_{m,j} \tag{3b}$$

are, respectively, the linear and nonlinear components of the incremental strain tensor between $C_1$ and $C_2$.

## Incremental Variational Equations

Assuming the current states of stresses and deformations of the body in $C_1$ (Fig. 1) are known, we seek an incremental variational expression in terms of the incremental state variables between $C_1$ and $C_2$. This expression is derived by obtaining the difference between the virtual work expressions of the body in $C_1$ and $C_2$, written with respect to the same reference state. Here,

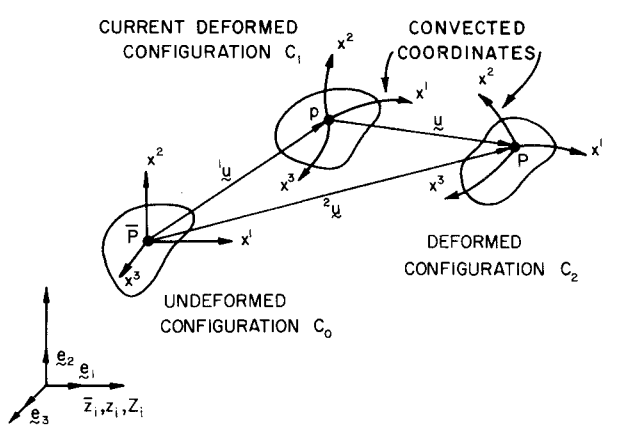


**Fig. 1 Configurations of a body (element) in its path of deformation.**

Presented as Paper 73-358 at the AIAA/ASME/SAE 14th Structures, Structural Dynamics, and Materials Conference, Williamsburg, Va., March 20–22, 1973; submitted April 9, 1973; revision received March 15, 1974.

Index categories: Structural Static Analysis; Thermal Stresses; Structural Stability Analysis.

* Research Specialist. Missiles Systems Division. Member AIAA.

† Group Engineer, Missiles Systems Division.

we choose the original configuration of the body as the reference state. In applying the results to derive the finite element equations, this choice of reference state eliminates the need to recompute a number of element matrices involving derivates and to update the nodal point coordinates as the geometry changes.

Neglecting the effect of body forces, the linearized form of the required incremental variational expression is given by[3]

$$\int_{\bar{a}} \hat{t}_i \, \delta u_i \, d\bar{a} = \int_{\bar{v}} {}^1s_{ij} \, \delta\eta_{ij} \, d\bar{v} + \int_{\bar{v}} s_{ij} \, \delta e_{ij} \, d\bar{v} \tag{4}$$

where $\bar{a}$ and $\bar{v}$ are, respectively, the boundary area and volume of the body in reference state $C_0$; ${}^1s_{ij}$ and $s_{ij}$ are, respectively, the total and incremental components of Piola-Kirchhoff stress tensors (in terms of the area and coordinates of the reference state), and

$$\hat{t}_i = \bar{t}_i + \bar{t}_m \, {}^1u_{i,m}, \; \bar{t}_i = s_{ij}\bar{n}_j \tag{5}$$

where $\bar{t}_i$ are the incremental components of surface traction in terms of the unit area and coordinates of the reference state, and $n_j$ are components of the unit outward normal to $\bar{a}$.

Expression (4) can be used to derive the element force-displacement relations in a direct incremental approach. However, the resulting solutions tend to diverge from the exact results depending on the step size and/or the degree of nonlinearity. One way of improving the quality of convergence is to add a residual loading term to the left-hand side of Eq. (4). This residual loading term can be obtained from the virtual work expression of the body in $C_1$, i.e.

$${}^1R_c = \int_{\bar{a}} {}^1\hat{t}_i \, \delta u_i \, d\bar{a} - \int_{\bar{v}} {}^1s_{ij} \, \delta e_{ij} \, d\bar{v} \tag{6}$$

where ${}^1\hat{t}_i = {}^1\bar{t}_i + {}^1\bar{t}_m \, {}^1u_{i,m}$, and ${}^1\bar{t}$ is the traction vector in $C_1$ per unit area $\bar{a}$. Note that in an exact mathematical sense, ${}^1R_c \equiv 0$; therefore, its inclusion does not jeopardize the equilibrium characteristics of expression (4).

## Incremental Constitutive Relations

Consistent with the incremental variational expression discussed in previous section, a nonisothermal elastic-plastic constitutive relation including the creep effects will be derived to relate the incremental Lagrangian strain tensor $\varepsilon_{ij}$ to the incremental Piola-Kirchhoff stresses $s_{ij}$. The derivation is based on the classical work of Green and Adkins,[4] Naghdi,[5] Prager,[6] and Odqvist.[7] In this development, initial isotropy is assumed; and the elastic and tangent moduli, the yield stresses, and $k$ (a measure of the size of loading surface) are assumed to be temperature dependent (see Fig. 2). Also, the material creep properties may vary as a function of time and temperature.

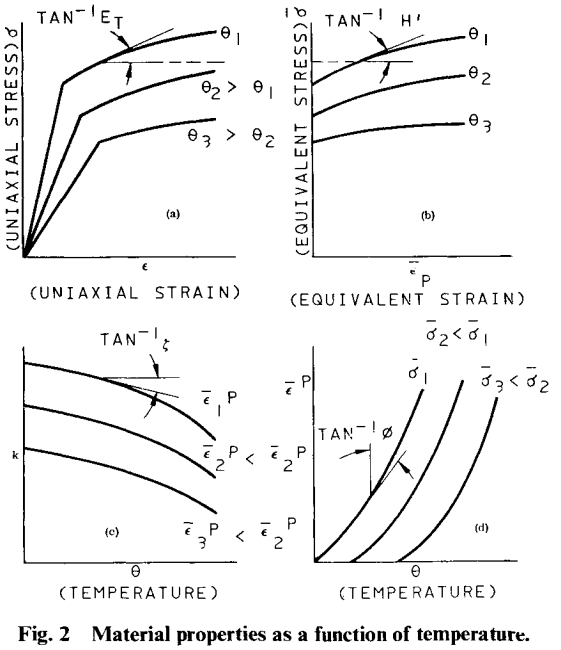


**Fig. 2 Material properties as a function of temperature.**

Assuming small strains, the incremental strain tensor $\varepsilon_{ij}$ is decomposed into elastic, $\varepsilon_{ij}{}^E$, thermal, $\varepsilon_{ij}{}^T$, plastic, $\varepsilon_{ij}{}^P$, and creep $\varepsilon_{ij}{}^C$, components; i.e.,

$$\varepsilon_{ij} = \varepsilon_{ij}{}^E + \varepsilon_{ij}{}^T + \varepsilon_{ij}{}^P + \varepsilon_{ij}{}^C \tag{7}$$

These components are defined through their respective constitutive relations as discussed in the following sections.

### The Elastic Component

$\varepsilon_{ij}{}^E$ is related to the stresses through the elastic material law,[4] i.e.,

$${}^1\varepsilon_{ij}{}^E = {}^1H_{ijmn} \, {}^1s_{mn} \tag{8}$$

where

$${}^1H_{ijmn} = [(1+\nu)/2{}^1E](\delta_{im}\delta_{jn} + \delta_{in}\delta_{jm}) - (\nu/{}^1E)\delta_{ij}\delta_{mn}$$

is the temperature-dependent elastic compliance tensor in $C_1$ and $\delta_{ij}$ is the Kronecker delta. By differentiating the above relation, the following incremental expression is obtained:

$$\varepsilon_{ij}{}^E = {}^1H_{ijmn}(s_{mn} - \zeta \, {}^1s_{mn}) \tag{9}$$

where $\zeta = d{}^1E/{}^1E$ and $d{}^1E \approx {}^2E - {}^1E$ is the change in elastic modulus due to a temperature change between $C_1$ and $C_2$. Here, it is assumed that for a small enough step between $C_1$ and $C_2$, all the differential increments at $C_1$ can be approximated by their respective incremental quantities between $C_1$ and $C_2$.

### The Thermal Component

$\varepsilon_{ij}{}^T$ is defined as

$$\varepsilon_{ij}{}^T = \alpha\delta_{ij}\theta \tag{10}$$

where $\alpha$ is the coefficient of thermal expansion, and $\theta = {}^2\theta - {}^1\theta$ is the temperature change between $C_1$ and $C_2$.

### The Plastic Component

$\varepsilon_{ij}{}^P$ is derived using von Mises nonisothermal yield function and its associated flow rule. Both isotropic and kinematic hardening laws will be considered.

In the case of isotropic hardening, the loading function is given by

$$F = ({}^3_2 \, {}^1t_{ij} \, {}^1t_{ij})^{1/2} - k({}^1\bar{\varepsilon}_p, {}^1\theta) = 0 \tag{11}$$

where‡ $F$ is the loading function and $k$ is a measure of strain hardening which is a function of temperature and equivalent plastic strain ${}^1\bar{\varepsilon}^P$ defined as

$${}^1\bar{\varepsilon}^P = \int_0^{{}^1\varepsilon_{ij}{}^P} d\bar{\varepsilon}^P \tag{12a}$$

$$d\varepsilon^P = ({}^2_3 \, d{}^1\varepsilon_{ij}{}^P \, d{}^1\varepsilon_{ij}{}^P)^{1/2} \tag{12b}$$

The functional form of $k = k({}^1\bar{\varepsilon}_p, {}^1\theta)$ may be obtained through the experimental data such as shown in Fig. 2c. In Eq. (11), ${}^1t_{ij} = {}^1s_{ij} - \frac{1}{3}\delta_{ij} \, {}^1s_{mm}$ is the deviatoric stress tensor in $C_1$. Using the normality condition

$$\varepsilon_{ij}{}^P = \lambda(\partial F/\partial {}^1s_{ij}) \tag{13}$$

where $\lambda$ is a positive scalar, given by[5]

$$\lambda = -[(\partial F/\partial {}^1s_{mn})s_{mn}\S + (\partial F/\partial {}^1\theta)\theta]/[(\partial F/\partial {}^1\varepsilon_{kl}{}^P)(\partial F/\partial {}^1s_{kl})] \tag{14}$$

together with the loading function (11), the incremental plastic strains are given by[8]

$$\varepsilon_{ij}{}^P = \frac{1}{H'}(3/2{}^1\bar{\sigma})^2 \, {}^1t_{ij} \, {}^1t_{mn} \, s_{mn} + (3\phi/2{}^1\bar{\sigma})\theta \, {}^1t_{ij} \tag{15}$$

where

$$H' = \partial k/\partial {}^1\bar{\varepsilon}^P = E\rho/(1-\rho), \phi = \partial {}^1\bar{\varepsilon}^P/\partial {}^1\theta$$

(see Fig. 2), $\rho = E_t/E$, and ${}^1\bar{\sigma} = ({}^3_2 \, {}^1t_{ij} \, {}^1t_{ij})^{1/2}$ is the equivalent stress in $C_1$.

In the case of kinematic hardening, the loading function is given by

$$F = [{}^3_2({}^1t_{ij} - {}^1\alpha_{ij})({}^1t_{ij} - {}^1\alpha_{ij})]^{1/2} - k_0({}^1\theta) = 0 \tag{16}$$

‡ Here and for the remainder of this paper the left superscript 1 is deleted on material constants.

§ Differential increments are approximated by finite increments between $C_1$ and $C_2$.

where ${}^1\alpha_{ij}$ is a tensor representing the total translation of the yield surface in the deviatoric stress space, and it is a measure of strain hardening, and $k_0$, which is temperature dependent, represents the size of the yield function. For a uniaxial state of stress $k_0 = \sigma_0({}^1\theta)$, where $\sigma_0$ is the uniaxial yield stress.

The increments of tensor ${}^1\alpha_{ij}$ between $C_1$ and $C_2$ is defined as

$$\alpha_{ij} = c(\varepsilon_{ij}{}^P + \zeta\, {}^1\varepsilon_{ij}{}^P) \tag{17}$$

where $c$ is a material constant which through a uniaxial tension test is given by

$$c = \tfrac{2}{3}H' = \tfrac{2}{3}E[\rho/(1-\rho)] \tag{18}$$

The second term on the right-hand side of Eq. (17) is included to account for a change in material constant $c$ due to a temperature change between $C_1$ and $C_2$.

Noting that $\partial F/\partial {}^1\alpha_{ij} = -\partial F/\partial {}^1s_{ij}$, when plastic flow occurs

$$dF = \frac{\partial F}{\partial {}^1s_{ij}}(d{}^1s_{ij} - d{}^1\alpha_{ij}) + \frac{\partial F}{\partial {}^1\theta}d{}^1\theta = 0 \tag{19}$$

which together with Eqs. (13) and (17) gives

$$\lambda = \left(\frac{\partial F}{{}^1s_{mn}}s_{mn} + \frac{\partial F}{\partial {}^1\theta}\theta - c\zeta\frac{\partial F}{\partial {}^1s_{ij}}{}^1\varepsilon_{ij}{}^P\right) \Big/ c\frac{\partial F}{\partial {}^1s_{kl}}\frac{\partial F}{\partial {}^1s_{kl}} \tag{20}$$

where the differential increments are approximated by the corresponding finite increments between $C_1$ and $C_2$. Using Eq. (16)

$$\partial F/\partial {}^1s_{mn} = (3/2\sigma_0)({}^1t_{mn} - {}^1\alpha_{mn}) \tag{21}$$

where $\sigma_0$ is the initial effective yield stress, and

$$\frac{\partial F}{\partial {}^1\theta} = -\frac{\partial k_0}{\partial {}^1\theta} = -\frac{\partial k_0}{\partial {}^1\bar{\sigma}}\frac{\partial {}^1\bar{\sigma}}{\partial {}^1\theta} - \frac{\partial k_0}{\partial {}^1\alpha_{ij}}\frac{\partial {}^1\alpha_{ij}}{\partial {}^1\theta} \tag{22}$$

Noting that

$k_0 = [\frac{3}{2}({}^1t_{ij} - {}^1\alpha_{ij})({}^1t_{ij} - {}^1\alpha_{ij})]^{1/2}$, $\partial {}^1\bar{\sigma}/\partial {}^1\theta = \partial k/\partial {}^1\theta = \xi = -\phi H'$ (Fig. 2), and

$$\partial {}^1\alpha_{ij}/\partial {}^1\theta \approx (c\zeta/\theta)\,{}^1\varepsilon_{ij}{}^P$$

Eq. (22) can be expressed as

$$\partial F/\partial {}^1\theta = H'[\phi + 3c\zeta/2\bar{\sigma}_o\theta({}^1t_{ij} - {}^1\alpha_{ij})\,{}^1\varepsilon_{ij}{}^P] \tag{23}$$

Introducing Eqs. (21) and (23) into Eq. (20) and the result into Eq. (13) gives

$$\varepsilon_{ij}{}^P = p_1({}^1t_{ij} - {}^1\alpha_{ij}) + p_2 B_{ijmn}s_{mn} \tag{24}$$

where

$$p_1 = \frac{3\phi}{2\sigma_0}\theta,\ p_2 = \frac{1}{H'}\left(\frac{3}{2\sigma_0}\right)^2 \tag{25a}$$

and

$$B_{ijmn} = ({}^1t_{ij} - {}^1\alpha_{ij})({}^1t_{mn} - {}^1\alpha_{mn}) \tag{25b}$$

Equation (24) would be equally applicable to the case of isotropic hardening, Eq. (15), if one considers $\alpha_{ij} = 0$ and replace $\sigma_0$ by ${}^1\sigma$.

## Loading/Unloading Criteria

Defining

$$L = (\partial F/\partial {}^1s_{ij})s_{ij} + (\partial F/\partial {}^1\theta)\theta \tag{26}$$

then loading into a plastic state would occur when $L > O$ and unloading from a plastic state into an elastic state would occur when $L < O$. When $L = O$, a state of neutral loading exists.[5] Substituting for the derivatives in Eq. (26)

$$L = (3/2{}^1\sigma)\,{}^1t_{ij}s_{ij} + H'\phi\theta \tag{27a}$$

in the case of isotropic hardening and

$$L = (3/2\sigma_0)({}^1t_{ij} - {}^1\alpha_{ij})s_{ij} + H'\phi\theta \tag{27b}$$

in the case of kinematic hardening.

### The Creep Component

$\varepsilon_{ij}{}^C$ is derived using the Norton-Odqvist steady-state creep law[7]

$$\dot{\varepsilon}_{ij}{}^C = \tfrac{3}{2}\,{}^1\beta^1\bar{\sigma}^{(n-1)}\,{}^1t_{ij} \tag{28}$$

where the dot denotes differentiation with respect to time, and ${}^1\beta$ and $n$ are the material creep constants—${}^1\beta$ may be time and temperature dependent. To find the creep strain increment in a finite time interval $\Delta t$, Eq. (28), is integrated to give

$$\varepsilon_{ij}{}^C = b_1\,{}^1t_{ij} + G_{ijmn}s_{mn} \tag{29}$$

where

$$b_1 = \tfrac{3}{2}\Delta t({}^1\beta + \tfrac{1}{2}\beta)\,{}^1\sigma^{(n-1)}$$
$$G_{ijmn} = b_2 T_{ijmn} + b_3 L_{ijmn}$$
$$b_2 = (3/2{}^1\sigma^2)(n-1)b_3$$
$$b_3 = \tfrac{3}{4}\Delta t({}^1\beta + \tfrac{2}{3}\beta)\,{}^1\sigma^{(n-1)}$$
$$T_{ijmn} = {}^1t_{ij}\,{}^1t_{mn}$$
$$L_{ijmn} = \tfrac{1}{2}(\delta_{im}\delta_{jn} + \delta_{in}\delta_{jm}) - \tfrac{1}{3}\delta_{ij}\delta_{mn},$$

and $\beta$ denotes an incremental change in creep constant between $C_1$ and $C_2$; i.e., $\beta = {}^2\beta - {}^1\beta$. Substituting Eqs. (9, 10, 24, and 29) in Eq. (7), the following incremental strain-stress relation is obtained.

$$\varepsilon_{ij} = R_{ijmn}s_{mn} - \zeta H_{ijmn}\,{}^1s_{mn} + (b_1 + p_1)\,{}^1t_{ij} - p_1\,{}^1\alpha_{ij} + \alpha\theta\delta_{ij} \tag{30}$$

where

$$R_{ijmn} = H_{ijmn} + G_{ijmn} + p_2 B_{ijmn} \tag{31}$$

For a finite element displacement formulation, the inverse of the previous relation, namely, the stress-strain relation, is required. For this, first the matrix $R$ in Eq. (31) should be inverted and then the required stress-strain relation will follow from Eq. (30). Although the above inversion can be accomplished through the use of matrix inversion routines, however, for economical reasons, it is more desirable to have the inverse readily available in a closed form. With some manipulations, $R^{-1}$ has been obtained which can be expressed as

$$C_{ijmn} = R^{-1}_{ijmn} = E_{ijmn} - a_1 L_{ijmn} - a_2 T_{ijmn} - a_3 A_{ijmn} + a_4 P_{ijmn} \tag{32}$$

where

$$E_{ijmn} = \mu(\delta_{im}\delta_{jn} + \delta_{in}\delta_{jm}) + \frac{2\nu\mu}{(1-2\nu)}\delta_{ij}\delta_{mn}$$

is the elastic modulus tensor, $\mu = E/[2(1+\nu)]$, $\nu$ is the Poisson's ratio

$$A_{ijmn} = {}^1\alpha_{ij}\,{}^1\alpha_{mn}$$
$$P_{ijmn} = {}^1\alpha_{ij}\,{}^1t_{mn} + {}^1t_{ij}\,{}^1\alpha_{mn},$$

and $a_1$, $a_2$, $a_3$, $a_4$ are scalars defined as

$$a_1 = 4\mu^2 b_3/(1 + 2\mu b_3)$$
$$a_2 = 2\mu/\psi\,\{3\mu h + 2\mu b_2[3\mu h\gamma(1-a_1) + e_0(1-3\mu h)]\}$$
$$a_3 = 6\mu^2 h/\psi(1-a_1)(1+2\mu n b_3)$$
$$a_4 = 6\mu^2 h/\psi[1 + 2\mu b_2\omega(1-a_1)]$$
$$\psi = e_0(1+2\mu b_3)(1-3\mu h)(1+2\mu n b_3) + 3\mu h[e_0(1+2\mu n b_3) - 2\mu b_2(\omega - e)^2]$$
$$h = (1-\rho)/\{\mu[3-(1-2\nu)\rho]\}$$
$$e = {}^1t_{ij}\,{}^1t_{ij} = \tfrac{2}{3}\,{}^1\bar{\sigma}^2,\ \omega = {}^1t_{ij}\,{}^1\alpha_{ij}$$
$$\gamma = {}^1\alpha_{ij}\,{}^1\alpha_{ij},\ \text{and}$$
$$e_0 = (e + \gamma - 2\omega) = \tfrac{2}{3}\bar{\sigma}_0{}^2$$

Introducing Eq. (32) into Eq. (30), the required stress-strain relation is obtained which may be expressed as

$$s_{ij} = C_{ijkl}\varepsilon_{kl} + \underline{\zeta\,{}^1s_{ij} - f_1\,{}^1t_{ij} - f_2\,{}^1\alpha_{ij}} - \underline{[E\alpha\theta/(1-2\nu)]\delta_{ij}} \tag{33}$$

where

$$f_1 = (\zeta/2\mu)(a_1 + ea_2 - \omega a_4) + (b_1 + p_1)(1 - a_1 - ea_2 + \omega a_4) + p_1(\omega a_2 - \gamma a_4) \tag{34a}$$

$$f_2 = (\zeta/2\mu)(\omega a_3 - ea_4) + [b_1 + p_1(ea_4 - \omega a_3)] + p_1(a_1 + \gamma a_3 - \omega a_4 - 1) \tag{34b}$$

Equation (33) is the stress-strain relation in a nine-dimensional stress space which includes thermo-elastic-plastic and creep effects. In the case of plasticity, it is applicable to both kinematic and isotropic hardening rules. For the latter, set ${}^1\alpha_{ij} = 0$ and $\omega = \gamma = 0$. If any of the above effects are absent, Eq. (33) may be modified by simply adjusting the coefficients in Eqs.

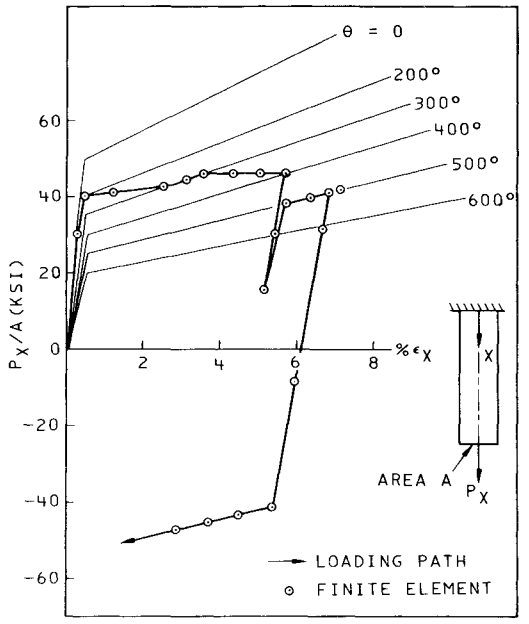


**Fig. 3 Uniaxial thermo-plastic problem (isotropic hardening).**

(32) and (33). For example, in case of no creep, set $b_1 = b_2 = b_3 = 0$ which gives $a_1 = 0$; in case of no plasticity, set $\rho = 1$, and $\phi = 0$ which gives $p_1 = a_3 = a_4 = f_1 = 0$; and in the case of thermo-elasticity, set $\rho = 1$, $\phi = b_1 = b_2 = b_3 = 0$ which results in $a_1 = a_2 = a_3 = a_4 = f_1 = f_2 = 0$, and

$$s_{ij} = E_{ijkl}\varepsilon_{kl} + \zeta^1 s_{ij} - [E\alpha\theta/(1-2\nu)]\delta_{ij} \tag{35}$$

Equation (33) may also be specialized for any subspace of the stress space (six space, plane stress, tension, etc.). For example, in the case of generalized plane stress where $s_{i3} = s_{3i} = 0$ and $\varepsilon_{\alpha 3} = 0$, Eq. (33) yields

$$s_{\alpha\beta} = \bar{C}_{\alpha\beta\gamma\delta}\varepsilon_{\gamma\delta} + \underline{\zeta^1 s_{\alpha\beta} - f_1\,{}^1t_{\alpha\beta} - f_2\,{}^1\alpha_{\alpha\beta} - [E\alpha\theta/(1-2\nu)]\delta_{\alpha\beta} - \chi_{\alpha\beta}} \tag{36}$$

where

$$\bar{C}_{\alpha\beta\gamma\delta} = C_{\alpha\beta\gamma\delta} - C_{\alpha\beta 33}C_{33\gamma\delta}/C_{3333} \tag{37a}$$

and

$$\chi_{\alpha\beta} = C_{\alpha\beta 33}[f_1\,{}^1t_{33} + f_2\,{}^1\alpha_{33} + E\alpha\theta/(1-2\nu)]/C_{3333} \tag{37b}$$

The underlined terms in Eqs. (36) and (33) can be treated as "initial stresses." In a finite element displacement formulation they will contribute to the element load vector, while the first term on the right-hand side will be used to compute the element stiffness matrix.

## Incremental Finite Element Equations

Following the standard finite element formulation procedure,[1] Eqs. (3, 4, 6, and 33) (or some special form of it) are used together with an assumed element expansion to derive the element equilibrium equations

$$[K_G + K_0]\{u\} = \{R\} \tag{38}$$

where $K_G$ (geometric stiffness matrix) and $K_0$ (ordinary stiffness matrix) are, respectively, obtained from the first and second integrals on the right-hand side of Eq. (4); $\{R\}$ is the element consistent load vector which includes the contributions due to mechanical loadings, "initial stresses" and the residual loading, Eq. (6), and $\{u\}$ is the element incremental displacement vector. The equilibrium equations of the discrete model are obtained by the direct assembly of the element equations (38). After imposing the boundary conditions, these equations are solved for the incremental displacements $u_i$. The incremental strains $\varepsilon_{ij}$ and stresses $s_{ij}$ are then computed using the appropriate element kinematical and constitutive relations. If applicable, the contributions of creep and thermal effects to $\varepsilon_{ij}$ are computed using Eqs. (10) and (29). If plastic flow occurs, i.e., $L > 0$ [see Eq. (26)], the plastic contribution to $\varepsilon_{ij}$ can be computed using Eq. (24). However, in the case of perfect plasticity, where $E_t = H' = \rho = 0$, the existing form of Eq. (24) is not admissible (it requires a division by zero). A more tractable version of this equation for such cases may be obtained by expressing $\varepsilon_{ij}^{P}$ in terms of incremental strains $\varepsilon_{ij}$ rather than stresses $s_{ij}$, this is done by substituting for $s_{mn}$ from Eq. (33).

## Numerical Examples

On the basis of the previous formulation, a general-purpose computer program called NEPSAP (Nonlinear Elastic-Plastic Structural Analysis Program) has been developed for the finite element analysis of three-dimensional structures. The program is capable of handling discrete models composed of beams, plates, shells, membranes, three-dimensional solids or any combination of them. So far NEPSAP has been successfully applied for the nonlinear bending and buckling analysis of a number of practical problems at Lockheed. To assess the accuracy and show some of the capabilities of NEPSAP, the following classical nonlinear problems have been solved and the results are compared with the analytical solutions available.

### Uniaxial Thermo-Elastic-Plastic Problem

Consider an axially loaded bar. The material property of the bar at different temperatures is shown in Fig. 3. Using one 3-*D* element and 20 load increments, the thermo-elastic-plastic behavior of the bar was investigated. The finite element results, together with the actual loading path (analytical solution) are shown in Fig. 3. As shown, a very good correlation between the two solutions is achieved.

### Elastic-Plastic Analysis of a Simply Supported Beam

The beam shown in Fig. 4 has a thickness of $h$, a width of unity and a length of $2L$. The material of the beam is assumed elastic, perfectly plastic with an elastic modulus of $E$ and a yield stress of $\sigma_y$. Under the action of a uniformly distributed lateral load $p$, the elastic-plastic behavior of the beam was investigated and the normalized load-deflection results are shown by the encircled points in Fig. 4. Also shown is the closed-form solution of this problem given in Ref. 9. The resulting agreement between the two solutions is quite satisfactory. For this problem a total of 20 load increments and 52 plane stress (4-node isoparametric) elements, 4 across the thickness and 13 along the half length, were used.

### Elastic-Plastic Analysis of an Infinitely Long Hollow Cylinder

Consider an infinitely long hollow cylinder with the internal and external radii of $a$ and $b$, respectively. The elastic, perfectly plastic solution of this cylinder with $b/a = 2$ and subjected to an internal pressure of $p_i$ is presented in Ref. 10. Assuming

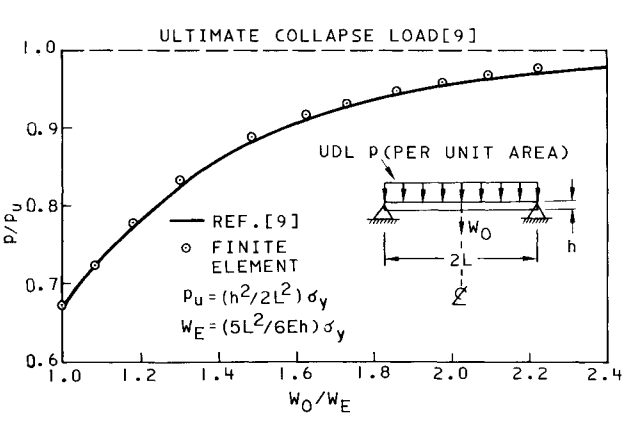


**Fig. 4 Load-deflection characteristics of an SS, elastic-plastic beam.**

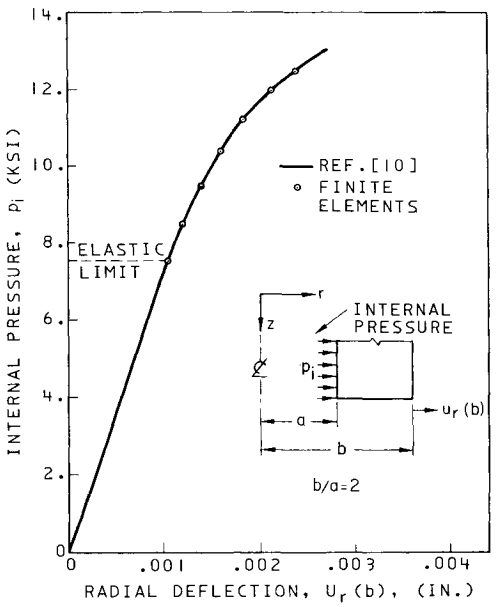


Fig. 5 Load-deflections of a hollow elastic-plastic cylinder.

$E = 8.67 \times 10^6$ psi, $\nu = 0.3$, $\sigma_y = 17320$ psi, and $b = 2a = 2$ in., the problem was analyzed using 10 axisymmetric solid elements (in radial direction) and 13 load increments. The finite element results together with the analytical solution[10] are shown in Figs. 5 and 6. Figure 5 shows the radial deflection at the outer radius as a function of internal pressure. As shown, the elastic limit is at $p_i = 7.5$ ksi, and at $p_i = 12.5$ ksi, the elastic-plastic boundary is at a radius of $r_p = 1.5a$. At this latter load, the distributions of hoop, $\sigma_\theta$, and radial, $\sigma_r$, stresses across the thickness are shown in Fig. 6. These results indicate a very good correlation between the finite element solution and that of Ref. 10.

### Elastic Large Displacements of an Infinite Plate Strip

This is a classical large displacement problem with a closed-form solution given in Ref. 11. The plate strip shown in Fig. 7 has a length of $L = 10$ in., a thickness of $h = 0.2$ in., and its dimension normal to the plane of paper is taken as infinity. The strip is subjected to a uniformly distributed load of $p$ (psi).

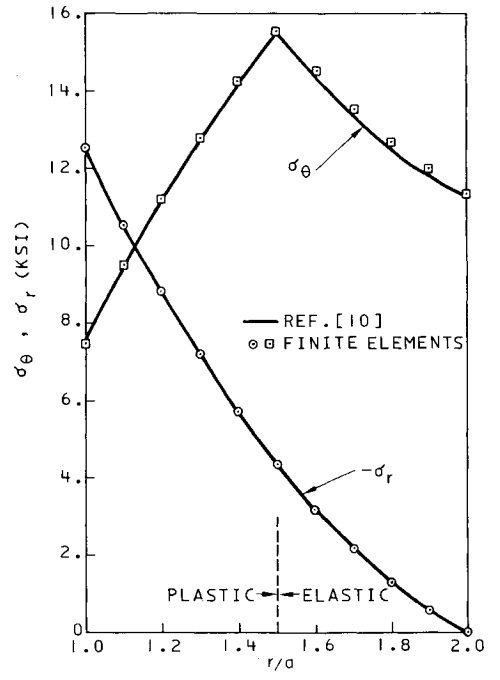


Fig. 6 Stresses in a hollow cylinder at $P_i = 12.5$ ksi.

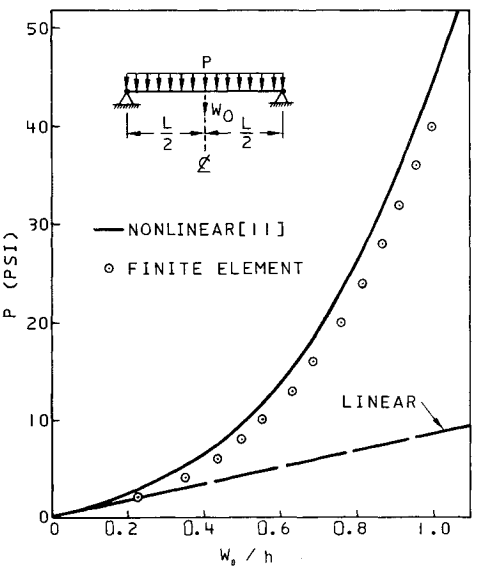


Fig. 7 Load-deflections of an infinite plate strip.

Assuming $E = 10^7$ psi and $\nu = 0.25$, the large displacement behavior of the strip was solved and the resulting finite element solution together with the closed-form solution is shown in Figs. 7 and 8. Figure 7 shows the vertical deflection at the center as a function of lateral load, and Fig. 8 shows the variations of maximum in-plane stresses, $\sigma_N$, and the maximum combined bending and in-plane stresses (at the center) vs the load. To obtain the finite element results, 4 isoparametric shell elements (16 nodes) and 13 load increments were used. With this rather crude model, the resulting agreement with the closed-form solution is quite satisfactory.

### Elastic Buckling of Composite Panels

The buckling strength of five $10 \times 10$ in. compression panels and four $18 \times 6$ in. shear panels were investigated. The compression panels are clamped at the loaded edges and clamped or simply supported at the other two edges. The shear panels are clamped on all four sides. These panels have a multilayered composite construction. Each layer is nominally 0.0051 in. thick and it is made of boron epoxy with the following orthotropic material properties: $E_{11} = 30.9 \times 10^6$ psi, $E_{22} = 2.5 \times 10^6$ psi, $G_{12} = 1.0 \times 10^6$ psi, and $\nu_{12} = 0.28$. In each panel, the material axes of the layers are oriented at different angles with respect to the axis of the load, but symmetrical about the midplane. The compression panels are composed of twenty layers and the shear panels sixteen layers.

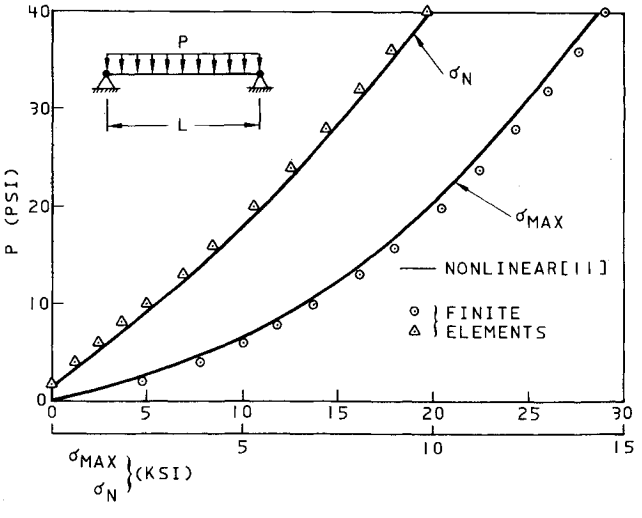


Fig. 8 Maximum and in-plane stresses as a function of load.

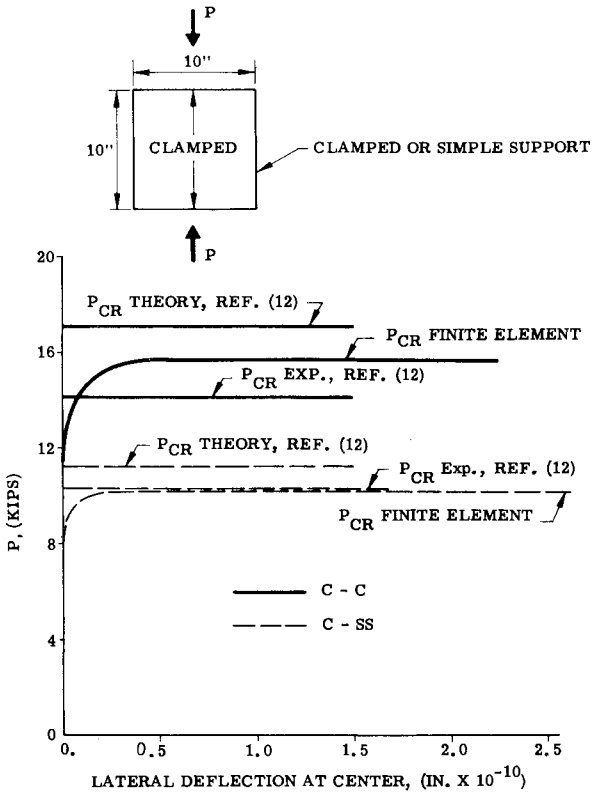


**Fig. 9 Compression buckling of composite panel no. 1.**

To determine the buckling loads of these panels a small lateral load (of the order of 1/10000 × buckling load) was applied at the center of each panel to trigger out-of-plane displacements. The loads were applied incrementally up to the buckling point. The criterion for buckling was either a sudden jump in the value of lateral deflection (see Fig. 9), or formation of negative term(s) on the diagonal of the structural stiffness matrix. Figure 9 shows the finite element solutions together with the experimental and theoretical results[12] for the compression panel 1. Similar results for the other panels were obtained. These results are summarized in Figs. 10 and 11. As shown, a very satisfactory correlation between the finite element solutions and the experimental and theoretical results reported in Ref. 12 is achieved. In this study, the compression and shear panels were, respectively, divided into 12 and 15 plate bending elements with multilayered construction.

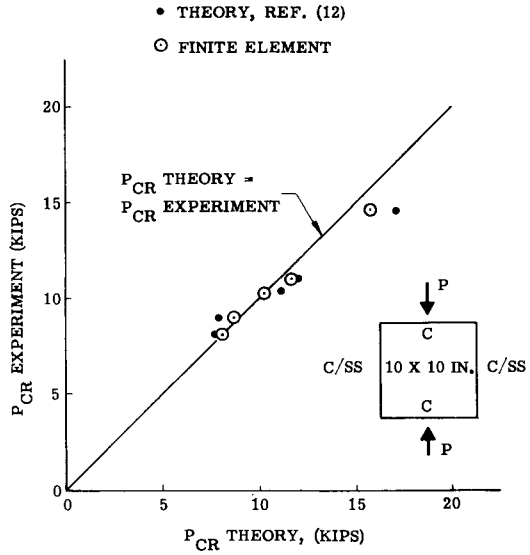


**Fig. 10 Compression buckling of composite panels.**

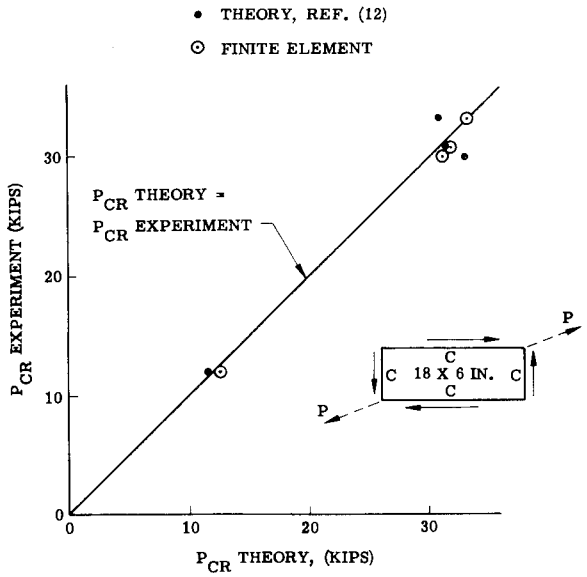


**Fig. 11 Shear buckling of composite panels.**

## Conclusions

Increasing use of new materials and applications of the structural components at severe loading and temperature environments has brought a greater demand for nonlinear analytical tools. One such tool, a general-purpose nonlinear finite element code, could be developed using the formulation presented. The main feature of this formulation is the development of an incremental constitutive relation for three-dimensional structures undergoing large nonisothermal elastic, plastic, and creep deformation. In this treatment, thermal effects and variation of material properties as a function of time and temperature are included. Using the above derivation together with an incremental Lagrangian displacement expression, a finite element computer program (NEPSAP) has been developed which contains different types of elements to handle geometries with a wide range of complexity. To illustrate some of the capabilities of this program, a number of test cases are solved and the results compared with the available closed-form solutions.

## References

[1] Zienkiewicz, O. C., *The Finite Element Method in Engineering Science*, McGraw-Hill, London, 1971.

[2] Oden, J. T., *Finite Elements of Nonlinear Continua*, McGraw-Hill, London, 1972.

[3] Yaghmai, S., "Incremental Analysis of Large Deformations in Mechanics of Solids with Application to Axisymmetric Shells of Revolution," CR-1350, June 1969, NASA.

[4] Green, A. and Adkins, A., *Large Elastic Deformation*, Oxford University Press, New York, 1960.

[5] Naghdi, P. M., "Stress-Strain Relations in Plasticity and Thermo-Plasticity," *Proceedings of the 2nd Symposium on Naval Structural Mechanics*, Brown Univ., Providence, R.I., 1960, pp. 121–167.

[6] Prager, W., "Non-Isothermal Plastic Deformation," TR 526(02)/4, 1957, Brown Univ., Providence, R.I., 1958, pp. 176–192.

[7] Odqvist, F., *Mathematical Theory of Creep and Creep Rupture*, Oxford University Press, New York, 1966.

[8] Sharifi, P. and Popov, E. P., "Nonlinear Buckling Analysis of Sandwich Shells," *Proceedings of the IASS Conference*, Calgary, Canada, July 1972, pp. 119–128.

[9] Prager, W. and Hodge, P. G., *Theory of Perfectly Plastic Solids*, Dover, New York, 1968.

[10] Hodge, P. G. and White, G. N., Jr., "A Quantitative Comparison of Flow and Deformation Theories of Plasticity," *Journal of Applied Mechanics*, Vol. 17, June 1950, pp. 180–184.

[11] Timoshenko, S. and Woinowsky-Krieger, S., *Theory of Plates and Shells*, 2nd ed., McGraw-Hill, New York, 1959.

[12] Suarez, J. A., "Advanced Composite Wing Structures, Stability Analysis of Advanced Filamentary Composite Panels," TR AC-SM-8087, May 1970, Grumman Aircraft Engineering Corp., Bethpage, N.Y.